

# Relaxing-Precessional Magnetization Switching

Hirofumi Morise and Shiho Nakamura

*Corporate R&D Center Toshiba Corporation*

## Abstract

A new way of magnetization switching employing both the spin-transfer torque and the torque by a magnetic field is proposed. The solution of the Landau-Lifshitz-Gilbert equation shows that the dynamics of the magnetization in the initial stage of the switching is similar to that in the precessional switching, while that in the final stage is rather similar to the relaxing switching. We call the present method the relaxing-precessional switching. It offers a faster and lower-power-consuming way of switching than the relaxing switching and a more controllable way than the precessional switching.

*Key words:* spin-transfer torque, magnetization switching, nanomagnet, Landau-Lifshitz-Gilbert equation, macrospin model  
*PACS:* 75.60.Jk, 85.75.-d, 75.75.+a

## 1. Introduction

The high-speed and low-power-consuming memories and data storage devices are expected in the current days. One of key technologies realizing such devices is the manipulation of the magnetization of a nanomagnet by use of the spin-transfer torque, which is proposed by Slonczewski [1] and Berger [2]. There, a spin-polarized current is introduced into an assembly of nanomagnets. The spin-polarized current, whose polarization direction is  $\hat{\mathbf{p}}$ , acts on a nanomagnet whose magnetization direction vector is  $\hat{\mathbf{m}}$ . The torque caused by the current is proportional to the vector  $\hat{\mathbf{m}} \times (\hat{\mathbf{p}} \times \hat{\mathbf{m}})$  [1]. It fluctuates the magnetization [3] or even reverse its direction [4].

To date, two different methods of the magnetization switching utilizing the spin-transfer torque have been proposed. The first method, which we call the relaxing switching, is more common.

There, the spin-polarization of the current which acts on the nanomagnet is almost parallel (or antiparallel) to the magnetization. The magnetization switches its direction according to the directions of the spin-polarization and the flow of the electrons. The switching dynamics is understood as a result of a relaxing process toward the equilibrium state. The main problem in the method for the application to memories is that it requires relatively high current density. The critical dc current,  $J_c$ , is of the order of  $10^7$  A/cm<sup>2</sup>. A naive explanation for the need of high current density is the following. The magnitude of the torque is small when the relative angle  $\theta$  between the magnetization of the nanomagnet and the spin-polarization of the conduction electrons is small, since  $|\hat{\mathbf{m}} \times (\hat{\mathbf{p}} \times \hat{\mathbf{m}})| = \sin \theta \approx \theta \ll 1$ .

Another problem is that the switching is slow. The results of the simulation indicates that the magnetization repeats the precessional motion un-

til it relaxes to the equilibrium state, demanding a time of the order of 1 ns in the case where the current is  $2-3J_c$  [5,6]. An experimental result show that at least four times larger current than the calculated critical current is needed to switch the magnetization in 100 ps [7]. In summary, the relaxing switching does not bring out the full potential ability of the spin-transfer torque.

The second method, which are called the precessional switching, has a possibility of overcoming such disadvantages [8,9]. There, the spin-polarization of the current is perpendicular to the magnetization of the nanomagnet. By taking such a configuration, it is possible to transmit the spin-transfer torque to the nanomagnet efficiently, and therefore realize the fast and low-power-consuming magnetization switching. However, it requires high-level controllability of the shape of the current pulse, including the pulse amplitude and the temporal width. Furthermore, the final state of the magnetization depends on its initial state, which indicates that the read-before-write is necessary. These disadvantages are due to the fact that the precessional switching employs the nonequilibrium state of the magnetization rather than the relaxation to the equilibrium state.

In the present work, an alternative method, which resolves the problems of the previous methods, is proposed. We call this new method the relaxing-precessional switching. It is different from the previous methods since it requires the simultaneous introduction of the spin-polarized current and the external magnetic field. The stable magnetization states under the spin-polarized current and the external magnetic field have been exhaustively studied in the previous work [10].

## 2. Phase diagram based on the linear stability

We consider a system composed of two ferromagnetic layers separated by a nonmagnetic layer. When the current in the direction perpendicular to the plane is introduced, the magnetization of the thinner (free) layer receives torques from the current, which is spin-polarized in the direction  $\hat{p}$ .

Here,  $\hat{p}$  denotes the magnetization direction vector of the thicker (pinned) layer. In addition, an external magnetic field  $\mathbf{H}_{\text{ext}}$  is applied in the in-plane hard axis direction. The magnetization direction vector  $\hat{m} = \mathbf{M}/M$  of the free layer obeys the following LLG equation:

$$\frac{d\hat{m}}{dt} = -\alpha\hat{m} \times \frac{d\hat{m}}{dt} + \gamma\hat{m} \times \mathbf{H}_{\text{eff}} + 2\pi M\gamma j\hat{m} \times (\hat{p} \times \hat{m}), \quad (1)$$

where

$$\mathbf{H}_{\text{eff}} \equiv \mathbf{H}_{\text{ext}} - 4\pi M m_x \mathbf{e}_x + H_K m_z \mathbf{e}_z, \\ j = \frac{1}{2\pi M\gamma} \frac{2\mu_B}{VM} \frac{gI_e}{|e|}. \quad (2)$$

Here,  $H_K$ ,  $\alpha$ ,  $\gamma$ ,  $\mu_B$ ,  $V$ ,  $I_e$ , and  $g$  denote the anisotropy field, the damping constant, the gyromagnetic ratio, the Bohr magneton, the volume of the free layer, the electric current, and the efficiency factor[1], respectively. The directions of  $\mathbf{H}_{\text{ext}}$  and  $\hat{p}$  are chosen so that  $\mathbf{H}_{\text{ext}} = H_{\text{ext}}\hat{e}_y$  and  $\hat{p} = \hat{e}_x$  respectively in the relaxing-precessional switching. The linear stability condition for the equilibrium states of the magnetization [10] allows one to draw the phase diagram for the stable magnetization states, which is shown in Fig. 1. We notice that there are bistable (B), monostable (M), and unstable (U) regions. In particular, we pay a special attention to the transition from a bistable region to a monostable region since it can be used as a switching mechanism. When the system undergoes such a transition by introducing the magnetic field and the spin-polarized current, the final direction of the magnetization is uniquely determined regardless of the initial direction. This gives the relaxing-precessional switching an advantage over the precessional switching. In addition, Fig.1 indicates that the direction of the magnetization can be changed to desirable direction between the two by choosing the direction of the spin-polarized current.

The critical current  $j_c^{\text{RP}}$ , needed for the reversal, is given by the boundary line between the bistable region and the monostable region. The monostable region appears because an equilibrium state, which was labeled as (S) in Ref.[10], become unstable above the boundary line. The analytical expression

for this line is obtained by solving the equation (see Appendix for the derivation):

$$H_{\text{ext}} = H_K \cdot h(j_c^{\text{RP}} \cdot 2\pi M/H_K), \quad (3)$$

where  $h(\xi)$  is a function defined by

$$h(\xi) \equiv \xi X(\xi)^{-3/2}(1 - 2X(\xi)), \quad (4)$$

and  $X(\xi)$  is a root of the equation :  $X^3 + \xi^2(X - 1) = 0$ . The asymptotic form of  $j_c^{\text{RP}}$  around  $H_{\text{ext}} = 0$  and that around  $H_{\text{ext}} = H_K$  are useful. They are written as

$$j_c^{\text{RP}}(H_{\text{ext}} \approx 0) = \frac{H_K}{2\pi M} \times \left\{ \frac{1}{2} - \frac{1}{\sqrt{2}} \frac{H_{\text{ext}}}{H_K} + \frac{1}{8} \left( \frac{H_{\text{ext}}}{H_K} \right)^2 + O \left( \frac{H_{\text{ext}}}{H_K} \right)^3 \right\} \quad (5)$$

and

$$j_c^{\text{RP}}(H_{\text{ext}} \approx H_K) = \frac{H_K}{2\pi M} \left[ \frac{2}{3} \left( 1 - \frac{H_{\text{ext}}}{H_K} \right) \right]^{3/2} \times \left\{ 1 - \frac{1}{12} \left( 1 - \frac{H_{\text{ext}}}{H_K} \right) + \frac{1}{864} \left( 1 - \frac{H_{\text{ext}}}{H_K} \right)^2 + O \left( 1 - \frac{H_{\text{ext}}}{H_K} \right)^3 \right\}, \quad (6)$$

respectively.

We notice that the critical current for the precessional switching [9,10]  $j_c^{\text{P}} = H_K/4\pi M$  coincides with  $j_c^{\text{RP}}(H_{\text{ext}} = 0)$  by setting  $H_{\text{ext}} = 0$  in eq.(5). As the field  $H_{\text{ext}}$  increases from zero, the critical current  $j_c^{\text{RP}}(H_{\text{ext}})$  decreases from this value. Taking  $H_{\text{ext}} = 0.5H_K$ , for example, we obtain  $j_c^{\text{RP}} = 0.37j_c^{\text{P}}$ . Furthermore, by taking  $\alpha = 0.01$  and  $H_K/4\pi M = 150\text{Oe}/1.8T = 0.0083$  as typical values, the critical currents of the relaxing-precessional, relaxing, and precessional switching are  $j_c^{\text{RP}} = 0.003$ ,  $j_c^{\text{R}}(=\alpha) = 0.01$ ,  $j_c^{\text{P}} = 0.008$ , respectively, which implies that the relaxing-precessional switching is the lowest-power consuming way among the three methods.

### 3. Numerical calculation of the LLG equation

As was discussed in the previous work [10], the final state which the magnetization obtains is be-

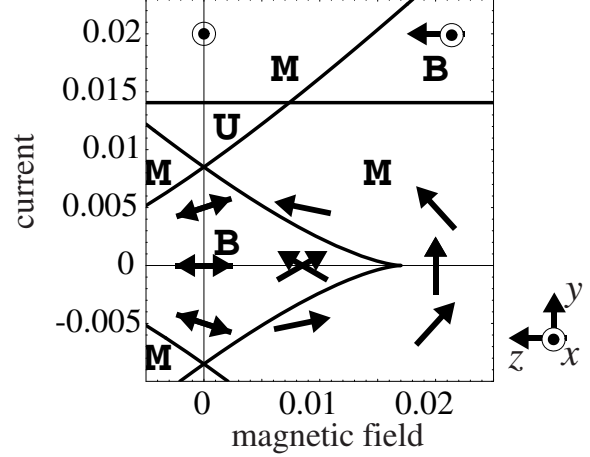


Fig. 1. Phase diagram of stable states based on the linear analysis. The horizontal and the vertical axes denote the dimensionless magnetic field  $H_{\text{ext}}/2\pi M$  and the dimensionless current  $j$ , respectively. We set  $H_K/2\pi M = 150\text{Oe}/0.9T = 0.017$ . Each of the arrows and the circles with dots represents the direction of a stable magnetization state. The former (latter) corresponds to the direction in (out of) the  $yz$ -plane. The labels “B”, “M”, and “U” denote bistable, monostable, and unstable regions, respectively.

yond the framework of the linear stability. Therefore, the numerical calculation of the LLG equation is necessary. In addition, switching speed is also discussed from the results. Here, it is assumed that the magnetic field is applied synchronously with the spin-polarized current.

Fig.2(a) shows a time-dependent solution of the LLG equation on the basis of the macrospin (single domain) model. In this example, the parameters are taken as  $H_{\text{ext}} = 0.5H_K$  and  $j = 0.003$ . It is worth comparing this solution with (b)that in the relaxing switching or (c)that in the precessional switching.

In the initial stage of the relaxing-precessional switching, the magnetization dislocates its direction from the initial one and begins precessional motion in response to the introduction of the spin-polarized current. This dynamic behavior is similar to that in the precessional switching. In the typical example of the relaxing-precessional switching shown in Fig.2(a), the reversal time is approximately 0.2 ns, which is almost the same as that in the precessional switching with a larger current

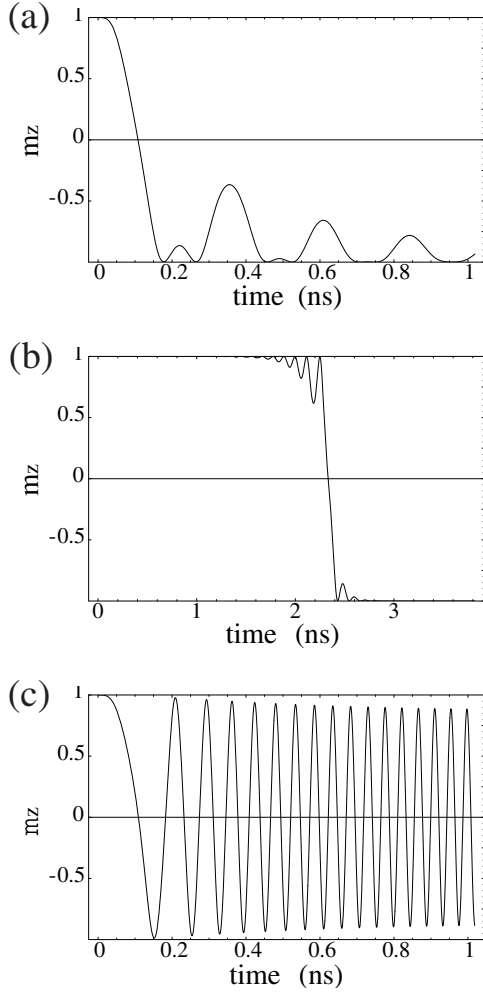


Fig. 2. The time evolution of  $m_z$  in (a) relaxing-precessional switching with  $H_{\text{ext}} = 0.5H_K$  and  $j = 0.003$ , (b) relaxing switching with  $j = 0.03$ , and (c) precessional switching with  $j = 0.01$ . We set  $H_K/2\pi M = 0.017$ .

[see Fig.2(c)].

Once the magnetization vector gets close to the opposite direction, it relaxes to the destination. The dynamics in this stage is very much different from that in the precessional switching and rather similar to that in the relaxing switching. This phenomenon is advantageous for the application to memories since it implies that any strict control of the temporal width of the current pulse is unnecessary.

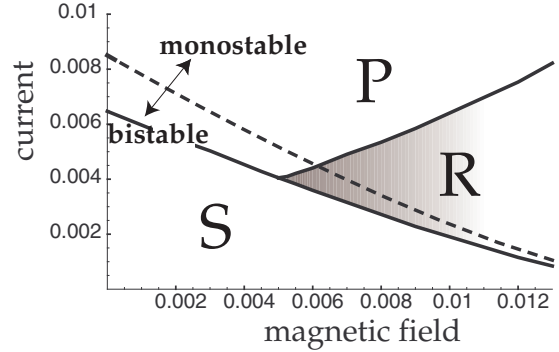


Fig. 3. Phase diagram of the dynamical behavior of the magnetization. We set  $H_K/2\pi M = 0.017$ . The definition of the axes is the same as that in Fig.1. The solid lines represent the boundary lines which distinguish the final states of the magnetization. In “S”, the magnetization stays in the neighborhood of the initial direction. In “P”, the magnetization continues a precessional motion. In “R”, the magnetization reverses its direction. The dashed line represents the boundary line between the monostable region and the bistable one, which have been shown in Fig.1.

#### 4. Ranges of the current and the magnetic field

The next task is to reveal the ranges of the spin-polarized current and the magnetic field which can be used as the relaxing-precessional switching. Here, we assume that the magnetic field is applied constantly in time.

Fig.3 is a phase diagram which illustrates the type of the dynamical behavior of the magnetization after the long-time introduction of the given magnitude of the spin-polarized current and that of the magnetic field. We have obtained this phase diagram by performing numerical calculations of the macrospin LLG equation. In the simulation, the current is assumed to rise instantaneously and be kept a constant value since then. The whole region is divided into one of the three regions labeled by “S”, “R”, and “P”, respectively. In the case where the point corresponding to the given values of the spin-polarized current and the magnetic field lies in the region S, the magnetization stays in the neighborhood of the initial direction during the introduction of the spin-polarized current. In the case

where it lies in the region R, the magnetization reverses its direction and does not return to the initial one after the spin-polarized current is introduced. In the case where it lies in the region P, the magnetization precesses and approaches neither the initial direction nor the opposite one. Therefore, the region R denotes the ranges of the spin-polarized current and the magnetic field which can be used as the relaxing-precessional switching. The dashed line represents the boundary between the monostable and the bistable states, which have been shown in Fig.1.

We have two remarks. First, the monostable region in Fig.1 does not overlap with the region S in Fig.3. This implies that the monostability is a sufficient condition of the switching. Thus, the analytical expression of the critical current obtained in Sec.2 overestimates the actual switching current.

Second, the ranges of the spin-polarized current and the magnetic field for the relaxing-precessional switching are limited to the triangle-shaped region shown as darkened one in Fig.3. When the spin-transfer torque is large, the switching is realized as a precessional switching rather than a relaxing-precessional switching. Therefore, too large spin-polarized currents are not suitable. Too large magnetic field is also undesirable for practical use. The magnetic field can be applied either by a current field or by a permanent magnet. In the former case, an additional power-consumption besides the current flowing through the multilayer must be taken into account while no additional power is consumed in the latter case.

To design a practical device including the read-out function, we can add a magnetic reference layer, whose magnetization direction is collinear to that of the free layer, to the system. In this system, the effect of the reference layer to the spin-transfer torque is negligible since the magnitude of the current used in the relaxing-precessional switching is too small to cause the relaxing switching as explained in the previous sections. Therefore, the adequate ranges of the magnetic field and the spin-polarized current discussed in this section are not affected by the addition of the reference layer.

## 5. Summary

In summary, we have proposed the relaxing-precessional magnetization switching, which utilizes both the spin-transfer torque and torque by a magnetic field. The present method can reverse a magnetization one order of magnitude faster with a current one order of magnitude lower than the conventional relaxing switching. In addition, it does not require strict control of the current pulse unlike the precessional switching.

## Appendix A. Derivation of eq.(3)

In this appendix, we present the derivation of the analytical expression (3) of the boundary line between the region M and B. We concentrate on the case where  $j > 0$  and  $0 < H_{\text{ext}} < H_K \ll 2\pi M$ . First, we parameterize the vector  $\mathbf{m}$ , which is on a unit sphere, in terms of the spherical coordinates  $\theta \in [0, \pi]$  and  $\phi \in [0, 2\pi)$  as

$$m_x = \sin \theta \cos \phi, \quad m_y = \sin \theta \sin \phi, \quad m_z = \cos \theta. \quad (\text{A.1})$$

The LLG equation (1) is rewritten as

$$\begin{aligned} \begin{pmatrix} \dot{\theta} \\ \dot{\phi} \end{pmatrix} &= \begin{pmatrix} f(\theta, \phi) \\ g(\theta, \phi) \end{pmatrix} \equiv \frac{\gamma}{1 + \alpha^2} \begin{pmatrix} 1 & \alpha \\ -\alpha & 1 \end{pmatrix} \begin{pmatrix} f_1 \\ f_2 \end{pmatrix} \\ f_1 &= \cos \phi (-4\pi M \sin \theta \sin \phi - H_K \sin \theta \sin \phi \\ &\quad + 2\pi M j \cos \theta) \\ f_2 &= (H_K \sin^2 \phi - 4\pi M \cos^2 \phi) \sin \theta \cos \theta \\ &\quad - H_{\text{ext}} \sin \theta - 2\pi M j \sin \phi \end{aligned} \quad (\text{A.2})$$

in the spherical coordinate. The equilibrium states are given by the solutions of the equations:  $f(\theta, \phi) = g(\theta, \phi) = 0$ . The solution which becomes unstable for large enough  $j > 0$  and  $H_{\text{ext}}$  is labeled as (S) in Ref.[10], which continuously changes into  $\mathbf{m} = -\mathbf{e}_y$  as  $H_{\text{ext}} \rightarrow \exists H < -H_K$  and  $j \rightarrow 0$ . The solution (S) is obtained by

$$H_K \sin \theta \cos \theta - H_{\text{ext}} \sin \theta - 2\pi M |j| = 0, \quad \sin \phi = \text{sgn}(j). \quad (\text{A.3})$$

In the following, we consider the existence of this solution and the stability of the state correspond-

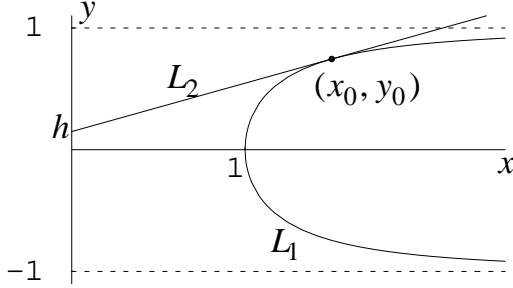


Fig. A.1.  $L_1 : y = \pm\sqrt{1-x^{-2}}$  and  $L_2 : y = (2\pi Mj/H_K)x + H_{\text{ext}}/H_K$ . When the two lines have common points, the equilibrium states corresponding to eq.(A.3) exist.

ing to this solution. The equation (A.3) is equivalent to

$$\pm\sqrt{1-x^{-2}} = (2\pi Mj/H_K)x + H_{\text{ext}}/H_K, \quad (\text{A.4})$$

if we set  $x \equiv 1/\sin\theta$ . Thus, the existence of the solution  $\theta$  is guaranteed when the two lines in the  $xy$ -plane,  $L_1 : y = \pm\sqrt{1-x^{-2}}$  and  $L_2 : y = (2\pi Mj/H_K)x + H_{\text{ext}}/H_K$ , share at least one point. Reminding that the gradient of the line  $L_2$  is positive, we see from Fig.A.1 that the two lines intersect when the  $y$ -intercept of the line  $L_2$  is smaller than some critical value  $h(2\pi Mj/H_K)$ , which is a function of the gradient of  $L_2$ . In other words, the existence condition is written as

$$\frac{H_{\text{ext}}}{H_K} \leq h \left( \frac{2\pi Mj}{H_K} \right). \quad (\text{A.5})$$

In the inequality (A.5), the equality holds when  $L_1$  and  $L_2$  are tangent to each other. In that case, the tangent point  $(x_0, y_0) \equiv (1/\sin\theta_0, \cos\theta_0)$  satisfies

$$y_0 = \sqrt{1-x_0^{-2}} = \frac{2\pi Mj}{H_K}x_0 + h \left( \frac{2\pi Mj}{H_K} \right), \quad (\text{A.6})$$

$$\begin{aligned} & \left. \frac{d}{dx} \sqrt{1-x^{-2}} \right|_{x=x_0} \\ &= \left. \frac{d}{dx} \left( \frac{2\pi Mj}{H_K}x + h \left( \frac{2\pi Mj}{H_K} \right) \right) \right|_{x=x_0}. \end{aligned} \quad (\text{A.7})$$

The condition (A.7) yields

$$x_0^{-6} + \left( \frac{2\pi Mj}{H_K} \right)^2 (x_0^{-2} - 1) = 0, \quad (\text{A.8})$$

which is rewritten as

$$\frac{2\pi Mj}{H_K} = \frac{x_0^{-3}}{\sqrt{1-x_0^{-2}}} = \frac{\sin^3\theta_0}{\cos\theta_0}. \quad (\text{A.9})$$

By introducing the function  $X(\xi)$ , which is defined as a root of the equation :  $X^3 + \xi^2(X-1) = 0$ , we have  $x_0^{-2} = X(2\pi Mj/H_K)$  and

$$h \left( \frac{2\pi Mj}{H_K} \right) = \frac{2\pi Mj}{H_K} \cdot X \left( \frac{2\pi Mj}{H_K} \right)^{-3/2} \times \left( 1 - 2X \left( \frac{2\pi Mj}{H_K} \right) \right). \quad (\text{A.10})$$

When  $H_{\text{ext}} < H_K \cdot h(2\pi Mj/H_K)$ ,  $L_1$  and  $L_2$  intersect each other at two points. Therefore, eq. (A.3) have two solutions  $\theta_<$  and  $\theta_>$ , which satisfy  $0 < \theta_< < \theta_0 < \theta_> < \pi/2$ .

In general, the equilibrium state is stable if all eigenvalues of the matrix:

$$L = \left( \begin{array}{cc} \partial f / \partial \theta & \partial f / \partial \phi \\ \partial g / \partial \theta & \partial g / \partial \phi \end{array} \right) \Bigg|_{f=g=0} \quad (\text{A.11})$$

have negative real parts, in other words,  $\text{tr}L < 0$  and  $\det L > 0$ . In the present system, the trace of  $L$  is negative because

$$\begin{aligned} \frac{1}{\alpha} \text{tr}L &= -2 + \frac{H_K}{2\pi M} (3 \cos^2\theta - 2) - 2 \cdot \frac{H_{\text{ext}}}{2\pi M} \cos\theta \\ &\leq -2 + \frac{H_K}{2\pi M} + 2 \cdot \frac{H_{\text{ext}}}{2\pi M} < 0. \end{aligned} \quad (\text{A.12})$$

Here, we have used the relation (A.3).

In contrast, the sign of the determinant of  $L$  cannot be determined automatically. Since  $\det L$  is calculated as

$$\det L = (1 + \alpha^2) \left( 2 + \frac{H_K}{2\pi M} \sin^2\theta + \frac{H_{\text{ext}}}{2\pi M} \cos\theta \right) \times \left( \frac{H_K}{2\pi M} \sin^2\theta - j \frac{\cos\theta}{\sin\theta} \right), \quad (\text{A.13})$$

we obtain

$$\begin{aligned} \text{sgn}(\det L) &= \text{sgn} \left( \frac{\sin^3\theta}{\cos\theta} - \frac{2\pi Mj}{H_K} \right) \\ &= \text{sgn} \left( \frac{\sin^3\theta}{\cos\theta} - \frac{\sin^3\theta_0}{\cos\theta_0} \right) = \pm 1 \iff \theta \gtrless \theta_0. \end{aligned} \quad (\text{A.14})$$

Thus, the equilibrium state corresponding to the solution  $\theta_>$  is always stable if it exists. In contrast, that corresponding to  $\theta_<$  is always unstable.

In summary, we have proved that there exist two equilibrium states under the condition  $H_{\text{ext}} \leq H_K \cdot h(2\pi Mj/H_K)$ . One of the equilibrium states is always stable if it exists. Namely, the above condition is not only the existence condition of an equilibrium state but also its stability condition.

## References

- [1] J. C. Slonczewski, *J. Magn. Magn. Mater.* 159 (1996) L1.
- [2] L. Berger, *Phys. Rev. B* 54 (1996) 9353.
- [3] M. Tsoi, A. G. M. Jansen, J. Bass, W.-C. Chiang, M. Seck, V. Tsoi, P. Wyder, *Phys. Rev. Lett.* 80 (1998) 4281.
- [4] E. B. Myers, D. C. Ralph, J. A. Katine, R. N. Louie, R. A. Buhrman, *Science* 285 (1999) 867.
- [5] J. Z. Sun, *Phys. Rev. B* 62 (2000) 570.
- [6] Z. Li, S. Zhang, *Phys. Rev. B* 68 (2003) 024404.
- [7] A. A. Tulapurkar, T. Devolder, K. Yagami, P. Crozat, C. Chappert, A. Fukushima, Y. Suzuki, *Appl. Phys. Lett.* 85 (2004) 5358.
- [8] A. D. Kent, B. Özyilmaz, E. del Barco, *Appl. Phys. Lett.* 84 (2004) 3897.
- [9] K. J. Lee, O. Redon, B. Dieny, *Appl. Phys. Lett.* 86 (2005) 022505.
- [10] H. Morise, S. Nakamura, *Phys. Rev. B* 71 (2005) 014439.